Quantum dots-nanogap metamaterials fabrication by self-assembly lithography and photoluminescence studies

Laxmi Narayan Tripathi,[1] Taehee Kang,[1] Young-Mi Bahk,[1] Sanghoon Han,[2] Geunchang Choi,[1] Jiyeah Rhie,[1] Jeeyoon Jeong,[1] and Dai-Sik Kim[1,*]

[1] *Center for Subwavelength Optics, Department of Physics and Astronomy, Seoul National University, Seoul 151-747, South Korea*

[2] *Photonic Systems Laboratory, School of EECS, Seoul National University, Seoul 151-744, South Korea*

[*] *dsk@phya.snu.ac.kr*

Abstract: We present a new and versatile technique of self-assembly lithography to fabricate a large scale Cadmium selenide quantum dots-silver nanogap metamaterials. After optical and electron microscopic characterizations of the metamaterials, we performed spatially resolved photoluminescence transmission measurements. We obtained highly quenched photoluminescence spectra compared to those from bare quantum dots film. We then quantified the quenching in terms of an average photoluminescence enhancement factor. A finite difference time domain simulation was performed to understand the role of an electric field enhancement in the nanogap over this quenching. Finally, we interpreted the mechanism of the photoluminescence quenching and proposed fabrication method of new metamaterials using our technique.

OCIS codes: (160.3918) Metamaterials; (220.3740) Lithography; (220.0220) Optical design and fabrication; (300.6280) Spectroscopy, fluorescence and luminescence; (260.2160) Energy transfer.

References and links

1. B. Metzger, M. Hentschel, T. Schumacher, M. Lippitz, X. Ye, C. B. Murray, B. Knabe, K. Buse, and H. Giessen, "Doubling the efficiency of third harmonic generation by positioning ITO nanocrystals into the hot-spot of plasmonic gap-antennas," Nano Lett. **14**(5), 2867–2872 (2014).
2. J. Lin, S.-H. Oh, H.-M. Nguyen, and F. Reitich, "Field enhancement and saturation of millimetre waves inside a metallic nanogap," Opt. Express **22**(12), 14402–14410 (2014).
3. T. Siegfried, L. Wang, Y. Ekinci, O. J. F. Martin, and H. Sigg, "Metal double layers with sub-10 nm channels," ACS Nano **8**(4), 3700–3706 (2014).
4. A. Toma, S. Tuccio, M. Prato, F. De Donato, A. Perucchi, P. Di Pietro, S. Marras, C. Liberale, R. Proietti Zaccaria, F. De Angelis, L. Manna, S. Lupi, E. Di Fabrizio, and L. Razzari, "Squeezing terahertz light into nanovolumes: nanoantenna enhanced terahertz spectroscopy (NETS) of semiconductor quantum dots," Nano Lett. **15**(1), 386–391 (2014).
5. X. Chen, H.-R. Park, M. Pelton, X. Piao, N. C. Lindquist, H. Im, Y. J. Kim, J. S. Ahn, K. J. Ahn, N. Park, D.-S. Kim, and S.-H. Oh, "Atomic layer lithography of wafer-scale nanogap arrays for extreme confinement of electromagnetic waves," Nat. Commun. **4**, 2361 (2013).
6. P. Pavaskar, J. Theiss, and S. B. Cronin, "Plasmonic hot spots: nanogap enhancement vs. focusing effects from surrounding nanoparticles," Opt. Express **20**(13), 14656–14662 (2012).
7. D. K. Gramotnev, M. G. Nielsen, S. J. Tan, M. L. Kurth, and S. I. Bozhevolnyi, "Gap surface plasmon waveguides with enhanced integration and functionality," Nano Lett. **12**(1), 359–363 (2012).

#235352 - $15.00 USD Received 4 Mar 2015; revised 21 May 2015; accepted 24 May 2015; published 29 May 2015

8. T. Siegfried, Y. Ekinci, H. H. Solak, O. J. F. Martin, and H. Sigg, "Fabrication of sub-10 nm gap arrays over large areas for plasmonic sensors," Appl. Phys. Lett. **99**(26), 263302 (2011).
9. D. Weber, J. Katzmann, F. Neubrech, T. Haertling, and A. Pucci, "Spectral tuning of IR-resonant nanoantennas by nanogap engineering," Opt. Mater. Express **1**(7), 1301–1306 (2011).
10. M. C. Hegg, M. P. Horning, T. Baehr-Jones, M. Hochberg, and L. Y. Lin, "Nanogap quantum dot photodetectors with high sensitivity and bandwidth," Appl. Phys. Lett. **96**(10), 101118 (2010).
11. H. Im, K. C. Bantz, N. C. Lindquist, C. L. Haynes, and S.-H. Oh, "Vertically oriented sub-10-nm plasmonic nanogap arrays," Nano Lett. **10**(6), 2231–2236 (2010).
12. D. R. Ward, F. Hueser, F. Pauly, J. Carlos Cuevas, and D. Natelson, "Optical rectification and field enhancement in a plasmonic nanogap," Nat. Nanotechnol. **5**(10), 732–736 (2010).
13. M. D. Fischbein and M. Drndic, "Sub-10 nm device fabrication in a transmission electron microscope," Nano Lett. **7**(5), 1329–1337 (2007).
14. Y. Sawai, B. Takimoto, H. Nabika, K. Ajito, and K. Murakoshi, "Observation of a small number of molecules at a metal nanogap arrayed on a solid surface using surface-enhanced Raman scattering," J. Am. Chem. Soc. **129**(6), 1658–1662 (2007).
15. D. R. Ward, N. K. Grady, C. S. Levin, N. J. Halas, Y. Wu, P. Nordlander, and D. Natelson, "Electromigrated nanoscale gaps for surface-enhanced Raman spectroscopy," Nano Lett. **7**(5), 1396–1400 (2007).
16. R. Negishi, T. Hasegawa, K. Terabe, M. Aono, T. Ebihara, H. Tanaka, and T. Ogawa, "Fabrication of nanoscale gaps using a combination of self-assembled molecular and electron beam lithographic techniques," Appl. Phys. Lett. **88**(22), 223111 (2006).
17. R. Esteban, A. G. Borisov, P. Nordlander, and J. Aizpurua, "Bridging quantum and classical plasmonics with a quantum-corrected model," Nat. Commun. **3**, 825 (2012).
18. A. M. Michaels, J. Jiang, and L. Brus, "Ag nanocrystal junctions as the site for surface-enhanced Raman scattering of single rhodamine 6g molecules," J. Phys. Chem. B **104**(50), 11965–11971 (2000).
19. N. J. Halas, S. Lal, W.-S. Chang, S. Link, and P. Nordlander, "Plasmons in strongly coupled metallic nanostructures," Chem. Rev. **111**(6), 3913–3961 (2011).
20. A. Cvitkovic, N. Ocelic, J. Aizpurua, R. Guckenberger, and R. Hillenbrand, "Infrared imaging of single nanoparticles via strong field enhancement in a scanning nanogap," Phys. Rev. Lett. **97**(6), 060801 (2006).
21. E. Cubukcu, S. Zhang, Y. S. Park, G. Bartal, and X. Zhang, "Split ring resonator sensors for infrared detection of single molecular monolayers," Appl. Phys. Lett. **95**(4), 043113 (2009).
22. C. Huck, F. Neubrech, J. Vogt, A. Toma, D. Gerbert, J. Katzmann, T. Hrtling, and A. Pucci, "Surface-enhanced infrared spectroscopy using nanometer-sized gaps," ACS Nano **8**(5), 4908–4914 (2014).
23. H.-R. Park, K. J. Ahn, S. Han, Y.-M. Bahk, N. Park, and D.-S. Kim, "Colossal absorption of molecules inside single terahertz nanoantennas," Nano Lett. **13**(4), 1782–1786 (2013).
24. H. Aouani, M. Rahmani, M. Navarro-Cia, and S. A. Maier, "Third-harmonic-upconversion enhancement from a single semiconductor nanoparticle coupled to a plasmonic antenna," Nat. Nanotechno. **9**(4), 290–294 (2014).
25. S. A. Maier, "Plasmonic field enhancement and sers in the effective mode volume picture," Opt. Express **14**(5), 1957–1964 (2006).
26. Y. C. Jun, R. Pala, and M. L. Brongersma, "Strong modification of quantum dot spontaneous emission via gap plasmon coupling in metal nanoslits," J. Phys. Chem. C **114**(16), 7269–7273 (2010).
27. D. J. Beesley, J. Semple, L. K. Jagadamma, A. Amassian, M. A. McLachlan, T. D. Anthopoulos, and J. C. deMello, "Sub-15-nm patterning of asymmetric metal electrodes and devices by adhesion lithography," Nat. Commun. **5**, 3933 (2014).
28. L. N. Tripathi, M. Praveena, P. Valson, and J. K. Basu, "Long range emission enhancement and anisotropy in coupled quantum dots induced by aligned gold nanoantenna," Appl. Phys. Lett. **105**, 163106 (2014).
29. Y.-L. Loo, D. V. Lang, J. A. Rogers, and J. W. P. Hsu, "Electrical contacts to molecular layers by nanotransfer printing," Nano Lett. **3**(7), 913–917 (2003).
30. J. R. Niskala, W. C. Rice, R. C. Bruce, T. J. Merkel, F. Tsui, and W. You, "Tunneling characteristics of Au-alkanedithiol-Au junctions formed via nanotransfer printing (NTP)," J. Am. Chem. Soc. **134**(29), 12072–12082 (2012).
31. D. Norris and M. Bawendi, "Measurement and assignment of the size-dependent optical spectrum in CdSe quantum dots," Phys. Rev. B **53**(24), 16338 (1996).
32. A. D. Yoffe, "Low-dimensional systems: quantum size effects and electronic properties of semiconductor microcrystallites (zero-dimensional systems) and some quasi-two-dimensional systems," Adv. Phys. **51**(2), 799–890 (2002).
33. M. Haridas, L. N. Tripathi, and J. K. Basu, "Photoluminescence enhancement and quenching in metal-semiconductor quantum dot hybrid arrays," Appl. Phys. Lett. **98**(6), 63305 (2011).
34. A. O. Govorov, J. Lee, and N. A. Kotov, "Theory of plasmon-enhanced forster energy transfer in optically excited semiconductor and metal nanoparticles," Phys. Rev. B **76**(12), 125308 (2007).
35. M. Alves-Santos, R. Di Felice, and G. Goldoni, "Dielectric functions of semiconductor nanoparticles from the optical absorption spectrum: the case of CdSe and CdS," J. Phys. Chem. C **114**(9), 3776–3780 (2010).
36. J. S. Ahn, T. Kang, D. K. Singh, Y.-M. Bahk, H. Lee, S. B. Choi, and D.-S. Kim, "Optical field enhancement of

#235352 - $15.00 USD Received 4 Mar 2015; revised 21 May 2015; accepted 24 May 2015; published 29 May 2015

1. Introduction

Plasmonic nanogap [1–16] has generated a lot of interest in the scientific community. Metallic nanogap has opened a new field of research called quantum plasmonics [17]. This interest in the nanogap research is generated since a metal nanogap provides high degree of confinement of an electric field between the gap of two metal surfaces [3, 5, 8, 11, 18, 19]. This field enhancement is well suited for surface enhanced Raman scattering [8, 11, 15], infra-red and THz sensing [9, 20–23] and optical non-linearities [24]. A metal insulator metal nanogap allows physical as well as effective mode volumes well below the diffraction limit in the gap material, even if there is a significant loss of energy inside the metal [25]. A strong modification of emission from the quantum dots (QDs) inside a nanogap is expected [26]. Preparation of a large scale, spacer based and few nanometer wide gaps have been recently demonstrated using Al_2O_3 [5] and a self-assembled monolayer [27]. The systematic incorporation of QDs using linker molecule has not been demonstrated yet.

Here, we demonstrate a wafer scale fabrication method, by combining the standard photolithography and a self-assembly, to manufacture Cadmium Selenide (CdSe) QDs-silver nanogap metamaterials. It is very difficult (time consuming) to fabricate 10 nm metal gaps, using focused ion beam (FIB), on a wafer-scale. Also, conventional e beam lithography requires a lot of time (many hours) to pattern the structure on a substrate while the photolithography does it rapidly (only limited by size of the wafer and a photo mask). The self-assembly of dithiols on a metal surface is also a rapid procedure. We have combined these two rapid procedures to fabricate the QDs inside the nanogap on a faster time scale. Although we have taken silver as a demonstration case, the self-assembly of thiols holds equally good for gold as well. Thus, an asymmetric metallic gap of silver and gold can also be fabricated. This shows the versatile nature of our approach to fabricate the QDs incorporated nanogap. To understand the nature of emission dynamics of QDs in the nanogap, we measured spatially resolved photoluminescence (PL) through a CdSe QDs-nanogap metamaterial and simulated the electric field profile across the CdSe QDs-nanogap using Finite Difference Time Domain (FDTD) method.

2. Experimental results and discussions

2.1. Sample fabrication

We prepared trioctylphosphine oxide (TOPO) capped CdSe QDs using a modified procedure [28]. A linker molecule of l-8 octanedithiol (OT) was used to exchange TOPO under heat and excess concentration of OT. The linker molecule has two sulfur ligands which covalently bind a metal (silver or gold) and a semiconductor [29] or between two metals [30]. Using these functionalized QDs we prepared QDs-nanogap metamaterials.

Figure 1 briefly explains the self-assembly lithography process of QDs-nanogap metamaterials. A cleaned and dried substrate of sapphire was used (Fig. 1(a)) for patterning the photoresist (PR) via photolithography (Fig. 1(b), appendix (b)). A 10 nm chrome layer was deposited over the PR pattern using thermal evaporator at the evaporation rate of 1 $\mathring{A}$ / sec (Fig. 1(c)), Followed by evaporation of first layer of 200 nm silver film (Fig. 1(d)). In fact, shape of first layer pattern decides the ring structures which can arbitrarily be of any shape. The nanogap width is decided by the size of the QDs and the chain length of a linker molecule. In this particular case, chain length of OT was 1.5 nm and core diameter of QDs was 4.5 ± 0.5 nm. Thus, the gap is expected to be 8 nm. We observed gap of 9 ± 1 nm. Further, evaporated silver (first layer) was dipped in acetone and sonicated at 150 W and 36 KHz for 2 minutes for lifting off the PR pattern (Fig. 1(e)). The sample was washed with Isopropyl alcohol and dried using N_2

#235352 - $15.00 USD Received 4 Mar 2015; revised 21 May 2015; accepted 24 May 2015; published 29 May 2015

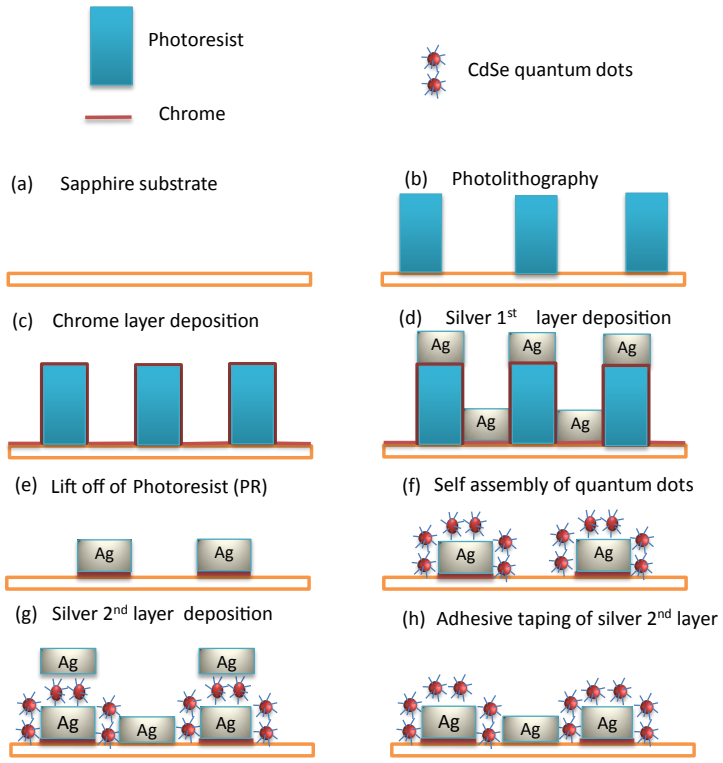

Fig. 1. Schematic of self-assembly lithography technique (cross sectional view): (a) A cleaned and dried substrate of sapphire; (b) PR pattern after using a mask aligner and UV lithography; (c) a chrome layer of 10 nm over the PR pattern; (d) a 200 nm thick silver film over the chrome layer using thermal evaporator; (e) first layer of metal pattern after lift off of PR; (f) self-assembled monolayer of QDs after dipping of first layer of metal into toluene solution of OT functionalized QDs; (g) second layer of metal deposited over self-assembled monolayer; (h) final QDs filled nanogap metamaterial after taping off second layer of silver.

gas. For self-assembly of QDs over the silver layer, the first layer metal pattern obtained after lift off was dipped in a functionalized QDs for one minutes and then washed by toluene (to remove unattached OT molecules) by dipping and shaking it for 3-4 sec, followed by drying using N_2 gas (Fig. 1(f)). A second layer of 100 nm and 190 nm of silver was deposited over it (Fig. 1(g)). Lower thickness of second layer is critical for successful taping of it. An equal or higher thickness of second layer resulted in failure of taping of the top layer due to direct contact between second layer of metal on the top and bottom of pattern. This contact provides a mechanical strength to the second layer sufficient for non-taping of it. Then a scotch tape [5] was used to tape off the top layer of metal. Thus, we get a vertical gap filled with a monolayer of QDs inside the metal nanogap (Fig. 1(h)).

Let us denote a metamaterial of dimensions, length of 300 μm, width of 50 μm, height of 200 nm and nanogap width of 9 ± 1 nm to be metamaterial R_1 (shown in Figs. 2(d) and 2(e)). Similarly, for dimensions, length of 20 μm, width of 20 μm, height of 200 nm and nanogap of width 9 ± 1 nm, to be metamaterial R_2 (shown in Figs. 2(b) and 2(c)). Figure 2 shows optical and electron microscopy characterizations of self-assembly lithography fabri-

#235352 - $15.00 USD Received 4 Mar 2015; revised 21 May 2015; accepted 24 May 2015; published 29 May 2015

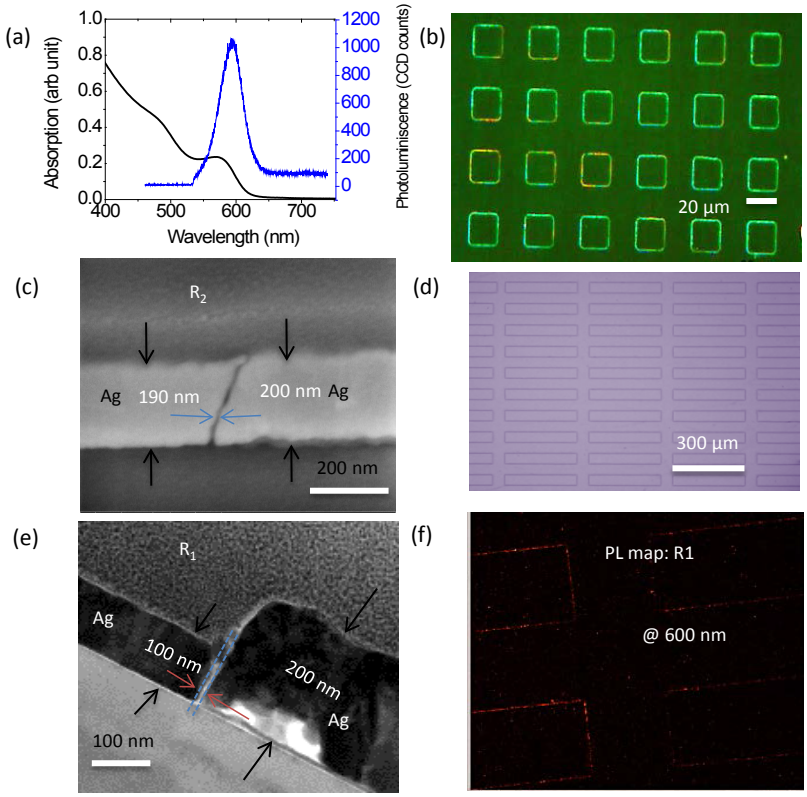

Fig. 2. Optical and electron microscopy characterization of QDs-nanogap metamaterials: (a) UV-Visible absorption spectra and PL from pristine QDs of mean size 4.5 ± 0.5 nm; (b) optical micrograph of R_2 through white light (unpolarized) transmittance showing ring of dimension ($20\ \mu m \times 20\ \mu m$); (c) Scanning electron microscope image of QDs-nanogap metamaterial R_2. Black arrows indicate the thickness of first (200 nm) and second layer (190 nm), while blue arrow indicates the QDs-nanogap; (d) optical micrograph of R_1 through white light reflection showing rectangular ring of dimension ($300\ \mu m \times 50\ \mu m$); (e) cross sectional transmission electron microscope image of QDs-nanogap metamaterial R_1. Black arrows indicate the thickness of first (200 nm) and second layer (100 nm), while red arrow indicates the QDs-nanogap further marked by doted blue line; (f) PL intensity map (in the reflection mode) of the QDs-nanogap metamaterial (R_1).

#235352 - $15.00 USD Received 4 Mar 2015; revised 21 May 2015; accepted 24 May 2015; published 29 May 2015

cated QDs-nanogap devices. The optical UV-visible absorption spectrum was recorded from QDs dispersed in toluene. A PL spectrum was recorded from a thin film of spin coated QDs in Polymethyl methacrylate (PMMA) matrix on a sapphire substrate with volume fraction of 4.4% at 6000 RPM for 60 seconds. CdSe QDs used were strongly quantum confined [31, 32] due to radius being less than bulk exciton Bohr radius of CdSe, 5.6 nm. A clear Stokes shift of 20 nm between the exciton absorption peak (574 nm) and emission peak (594 nm) can be seen from Fig. 2(a). White light transmission image of self-assembly lithography patterned QDs and 10 nm gaps between silver pattern of R_2 devices is shown in Fig. 2(b). Light passing through it traces the rings which are nothing but lithographically patterned QDs-nanogap structures. White light reflection image of self-assembly lithographically patterned metamaterial R_1 device is shown in Fig. 2(d). Cross sectional electron microscope image for the two metamaterials, R_2 and R_1 are shown in Fig. 2(c) and Fig. 2(e) respectively. A reflection mode optical micrograph of PL intensity from metamaterial R_1 at emission wavelength of QDs (600 nm) is shown in Fig. 2(f). A confocal microscope (Carl Zeiss microscopy, GmbH, Germany with 40 X water immersion objective) at 488 nm excitation was used for the measurement. We can see a clear contrast of PL intensity. The line of higher emission intensity represents the QDs self assembled on the first layer of silver above QDs-nanogap region.

2.2. *Photoluminescence transmission measurements on a QDs-nanogap metamaterial*

In the QDs-nanogap metamaterial, 200 nm thick silver film reduces the background signals in the transmission mode and only the nanogap region is allowed to transmit the incident beam. This is an advantage for an experimentalist provided by thin film metal nanogap as opposed to nanogaps formed by a bow tie or nanoparticles. To understand the nature of PL (quenching or enhancement) we measured PL spectra in the transmission mode.

Figure 3 summarizes the PL spectra collected in transmission mode. As shown in a schematic diagram of the set-up used for the transmission measurement (Fig. 3(a)), we used a super continuum laser (Fianium, SC-400) with acoustic-optic tunable filter (AOTF) to single out 514 nm for excitation source. Incident light was focused to single nanogap through 100 X objective lens (Nikon CF Plan, N.A., 0.8) with a spot size about 1 μm and collected by a 60 X objective lens (Olympus Uplan Apo, N.A., 0.9). Transmitted PL was detected by a spectrometer (Princeton Instrument SP 2300i) using 300 mm groove, 500 nm blazed grating, equipped with nitrogen-cooled CCD array. A 532 nm long pass filter was used to block the incident laser line in the emission spectra. All spectra shown in Fig. 3(b) were collected using a 500 μW laser focused over the nanogap and using an integration time of 60 sec from various locations of the nanogap. Inset of Fig. 3(b) shows a PL spectrum collected from a pristine QDs-PMMA thin film using 1.6 μW laser power with an integration time of 1 sec.

We observed low intensity PL emission from the nanogap as compared to that from pristine QDs-PMMA thin film. We had to increase the incident laser power by a factor of 312.5 and increase the integration time by a factor of 60 to collect the PL through the nanogap. The volume fraction of QDs in the nanogap was 24% as opposed to that in QDs-PMMA thin film which was 4.4%. To understand the nature of PL (whether there is quenching or enhancement), let us define an *average PL enhancement factor*, F_{av}^{Pl} from the QDs-nanogap metamaterial by

$$F_{av}^{Pl} = \left(\frac{I_{gap}}{I_{ref}}\right) \times N \tag{1}$$

where N is normalization factor defined by

$$N = \left(\frac{f_{ref}}{f_{gap}}\right) \times \left(\frac{t_{ref}}{t_{gap}}\right) \times \left(\frac{P_{ref}}{P_{gap}}\right) \times \left(\frac{A_{ref}}{A_{gap}}\right) \tag{2}$$

#235352 - $15.00 USD Received 4 Mar 2015; revised 21 May 2015; accepted 24 May 2015; published 29 May 2015

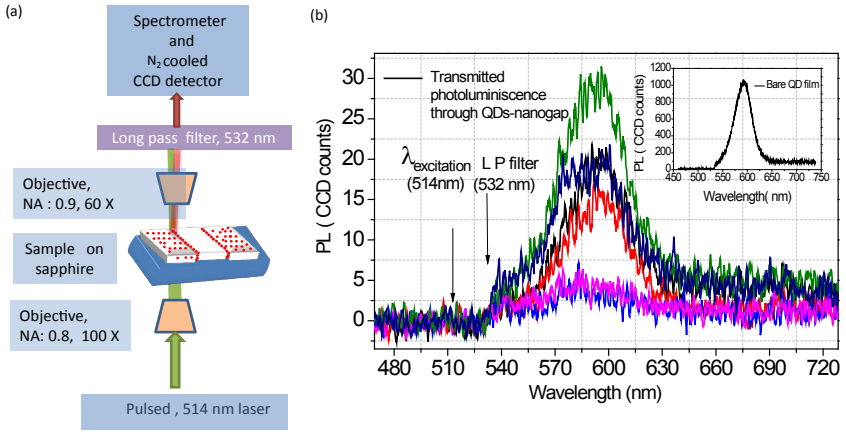

Fig. 3. Photoluminescence measurement through the QDs-nanogap metamaterial: (a), Photoluminescence measurement set-up (b), Photoluminescence spectra though the QDs-nanogap metamaterial R_2. Inset: Photoluminescence from the pristine QDs-PMMA thin film. Here, NA: numerical aperture and CCD: Charge coupled device, LP: long pass filter. $\lambda_{excitation}$: excitation wavelength. Bare QD film refers to CdSe QDs-PMMA thin film.

where I_{gap}, I_{ref} are the average PL intensity counts from the QDs-nanogap metamaterial and the QDs thin film respectively; f_{gap}, f_{ref}: volume fraction of QDs in nanogap and in the QDs-PMMA thin film respectively; t_{gap}, t_{ref}: Integration time used for the QDs-nanogap metamaterial and QDs-PMMA thin film respectively ; P_{gap}, P_{ref}: Incident power of 514 nm laser used for exciting QDs-nanogap metamaterial and QDs-PMMA thin film respectively; A_{gap}, A_{ref}: Area of the sample exposed to laser beam for the QDs-nanogap metamaterial and QDs PMMA thin films respectively. We have taken the area of the nanogap A_{gap} to be $(1\ \mu m \times 0.01\ \mu m)$ while the area of the beam spot over the QDs-PMMA thin film was calculated to $(\pi \times (0.5)^2)$ $(\mu m)^2$. Using these values and the experimental parameters, the value of N turns out to be 0.02. Considering 20 as the average PL counts from the QDs-nanogap metamaterials and 1000 that from pristine QDs-PMMA thin film. The average PL enhancement factor, F_{av}^{Pl} is found to be 4×10^{-4}, which is reasonably low, the reason for this low enhancement factor can be a non-radiative energy transfer from the QDs to the silver metal [33, 34].

2.3. Two dimensional FDTD simulation of field enhancements for QDs-nanogap slit

To understand the effect of an electric field enhancement over PL intensity at the excitation wavelength of 514 nm, we simulated the electric field distribution pattern inside the nanogap region of nanoslit using two dimensional FDTD method (Fig. 4). For this simulation, a non-uniform grid (minimum grid size: 0.1 nm) was considered. Slit width was taken to be 8 nm (5 nm for QD diameter and 1.5 + 1.5 nm for linker molecule chain length on both side of the QD). The slit thickness was taken to be 200 nm while slit material was taken to be silver with refractive index at 514 nm as 0.14077 and absorption coefficient at 514 nm to be 2.9110. The dielectric function of CdSe QDs [35], was taken to be 8.0 + 1.3 i. Refractive index at 514 nm of linker molecule was taken to be 1.5. Index of refraction of sapphire substrate was assumed to be 1.77. The average electric field enhancement in the QDs region was found to be 0.16. It is noteworthy that a PL can be enhanced due to increased excitation rate of QDs [33] in the region of hot spots created by an enhanced electric field in the nanogap. Since, there is no field enhancement inside the QDs-nanogap regions at the incident wavelength, the field enhancement

#235352 - $15.00 USD Received 4 Mar 2015; revised 21 May 2015; accepted 24 May 2015; published 29 May 2015

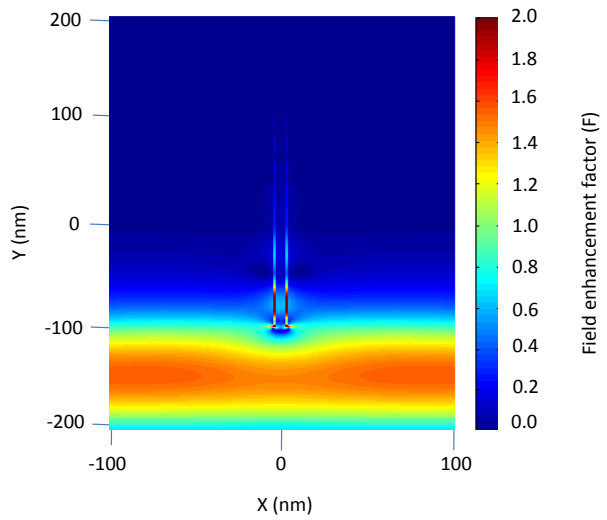

Fig. 4. 2D FDTD simulation of the QDs - silver nanogap of an infinite slit: XY cross sectional view of the electric field enhancement factor profile at 514 nm for the metamaterial R_2. Y is the direction of incident plane wave and X that of its polarization.

at the excitation wavelength cannot increase the PL intensity from the QDs-nanogap metamaterials. Further, from Fig. 4 we can see that there is an electric field enhancement gradient through the nanogap region, i.e the enhancement factor has the maximum value at the entrance side of the slit while it is minimum on the exit side. In the simulation, the enhancement factor was calculated by dividing the electric field value in the QDs-nanogap metamaterial with incident field value through the bare sapphire substrate.

3. Conclusion

We have demonstrated the self-assembly lithography technique for preparation of CdSe QDs-Silver nanogap metamaterials. Since thiol linker molecule works good for both silver (Ag) and gold (Au), these techniques can be applied to fabricate Au-QDs-Au and Au-QDs-Ag nanogap metamaterials as well. Besides, a self-assembly does not depend on the shape of the ring, this method will also be applicable to fabricate arbitrary shape of the nanogap. Thus, it presents a versatile method of QDs embedded nanogap fabrication. We also measured highly quenched PL spectra in the transmission mode. This quenching of PL in the nanogap at the incident wavelength is supported by FDTD results. Recently, Ahn et al. [36] have shown that a field enhancement from the metal nanogap will be significantly large (about 10) at near infra-red frequency and at smaller gap width. Thus, a sub-nanometre gap-width with QDs on the top of it will be an interesting sample for studying the decay dynamics of the QDs under strong fields. The detailed decay dynamics of QDs inside the nanogap can further be studied using time correlated single photon counting (TCSPC) methods. Further, we hope that these QDs-nanogap metamaterials will find many applications in cavity quantum electrodynamics, molecular sensing, nanogap quantum dot photo detectors etc.

#235352 - $15.00 USD Received 4 Mar 2015; revised 21 May 2015; accepted 24 May 2015; published 29 May 2015

4. Appendix

4.1. Functionalization of QDs

TOPO capped CdSe QDs were cleaned twice with methanol and toluene via centrifugation for removing the excess TOPO. Further, 500 μl (a typical concentration of 1.1 mg/ml) of thus cleaned TOPO CdSe QDs in toluene was heated for 5 min and then mixed with 500 μl of OT. The whole solution thus obtained was heated at 150 °C for 5 min. The colour of solution did not change after the exchange. Further, this solution did not show any phase separation.

4.2. Photo lithography

A sapphire substrate was cut into 1 cm by 1 cm piece. It was cleaned using sonication at 150 W and 36 kHz for 5 minutes each in acetone and Isopropyl alcohol (IPA) respectively and finally was dried using N_2 gas. A PR adhesive, Hexamethyldisilazane (HDMS) in Xylene was spin coated at 4000 RPM for 60 seconds over the sapphire substrates. The substrate was then baked for 60 sec at 90 °C. A PR (AZ 5206) was spin coated at 6000 RPM for 60 sec and baked for 90 sec. A mask aligner with chrome mask of desired micro-structure (300 μm by 50 μm for $R_1$and 20 μm by 20 μm for R_2) was selected and stamped over the sample by approaching the sample onto the mask. This was followed by first UV exposer for 6 sec then baked at 115 °C for 2 minutes. Again second UV exposer for 40 seconds without mask was performed. Then developed using MIF 300 for 3 seconds followed by rinsing with DI water. The developed pattern was checked for clean image (with reflected rainbow colours at the edges), a proof of fully developed pattern. If necessary, the development process was repeated for one or more times. A note for caution is that an excessive development process led to washing of the PR patterns.

Acknowledgements

Laxmi Narayan Tripathi acknowledges Brain Korea 21 Plus 2014 for the post-doctoral fellowship. The experimental work was supported by the National Research Foundation of Korea (NRF) grant funded by the Korea government (MSIP) (No. 2008-0061906, 2005-0093838, 2008-00580) and the Brain Korea 21 Plus Project in 2014. We thank Prof Sungchul Hohng, department of physics and astronomy, Seoul national university, Seoul, Korea for allowing using research facilities from his lab.

#235352 - $15.00 USD Received 4 Mar 2015; revised 21 May 2015; accepted 24 May 2015; published 29 May 2015